HHS Public Access

Author manuscript

Opt Lett. Author manuscript; available in PMC 2015 May 13.

Published in final edited form as:

Opt Lett. 2015 March 15; 40(6): 1113–1116.

Assessing Microstructures of the Cornea with Gabor-Domain Optical Coherence Microscopy: Pathway for Corneal Physiology and Diseases

Patrice Tankam[1,2,*], **Zhiguo He**[3], **Ying-Ju Chu**[4], **Jungeun Won**[1,4], **Cristina Canavesi**[5], **Thierry Lepine**[6], **Holly B. Hindman**[7], **David J. Topham**[8], **Philippe Gain**[3], **Gilles Thuret**[3,9], and **Jannick P. Rolland**[1,2,4,5]

[1]The Institute of Optics, University of Rochester, 275 Hutchinson Road, Rochester, New York 14627, USA

[2]Center for Visual Science, University of Rochester, 601 Elmwood Avenue, Rochester, NY 14642, USA

[3]Corneal Graft Biology, Engineering and Imaging Laboratory, EA 2521, SFR143, Faculty of Medicine, Jean Monnet University, 15 Rue Ambroise Paré, F 42023 Saint-Etienne Cedex 2, FRANCE

[4]Department of Biomedical Engineering, University of Rochester, 275 Hutchinson Road, Rochester, New York 14627, USA

[5]LighTopTech Corp., 150 Lucius Gordon Dr., Ste 115, West Henrietta, NY 14586, USA

[6]Université de Lyon, CNRS, Laboratoire Hubert Curien (UMR 5516), 18 rue Benoît Lauras F-42000, Saint-Etienne, France

[7]Department of Ophthalmology, University of Rochester Medical Center, 601 Elmwood Ave, Rochester, NY 14642, USA

[8]Department of Microbiology and Immunology, University of Rochester Medical Center, 601 Elmwood Ave, Rochester, NY 14642, USA

[9]Institut Universitaire de France, Boulevard Saint-Michel, Paris, FRANCE

Abstract

Gabor-domain optical coherence microscopy (GD-OCM) was applied *ex vivo* in the investigation of corneal cells and their surrounding microstructures with particular attention to the corneal endothelium. Experiments using fresh pig eyeballs, excised human corneal buttons from patients with Fuchs' endothelial dystrophy, and healthy donor corneas were conducted. Results show in a large field of view (1 mm × 1 mm) high definition images of the different cell types and their surrounding microstructures through the full corneal thickness at both the central and peripheral locations of porcine corneas. Particularly, an image of the endothelial cells lining the bottom of the cornea is highlighted. As compared to healthy human corneas, the corneas of individuals with

*Corresponding author: ptankam@optics.rochester.edu.

Fuchs' endothelial dystrophy show characteristic microstructural alterations of the Descemet's membrane and increased size and number of keratocytes. The GD-OCM based imaging system developed may constitute a novel tool for corneal imaging and disease diagnosis. Also, importantly, it may provide insights into the mechanism of corneal physiology and pathology, particularly in diseases of the corneal endothelium.

The cornea is the outermost component of our visual system and plays key roles such as protecting the eye against germs, dust and harmful matter, as well as refracting the incoming light in the eye. The cornea is composed of several layers (the epithelium, the Bowman's layer, the stroma, and the endothelium and its basement membrane – Descemet's membrane (DM) –), each playing distinct and important functions. One of the most important characteristics of the cornea is its perfect transparency due to the hyper-regular organization of the collagen fibrils in the stroma and maintained by the deturgescence state of the cornea [1]. The corneal endothelium is the innermost corneal layer made of a monolayer of cells whose primary function is to maintain the corneal transparency [2] by pumping excess fluid out of the stroma to aqueous humor. Dysfunction of endothelial cells (ECs) leads to greater hydration of the corneal stroma, which can cause irreversible corneal edema, itself causing opacity and blindness. Corneal transplantation is nowadays the only therapy available to treat corneal opacity caused by EC dysfunction, such as Fuchs' endothelial dystrophy (FED). One challenge in biomedical imaging is providing cellular-resolution images of deep layers in tissues, up to millimeters deep, thus reducing the need of biopsy and allowing *in-vivo* investigation of disease mechanisms. This is particularly important for the cornea, for which biopsy is deleterious. Specular Microscopy (SM) has been used to image ECs and to evaluate endothelial cell attrition following various types of intraocular surgery or treatment [3–6]. Particularly, SM is used by ophthalmologists to evaluate endothelial cell density (ECD) and diagnose corneal cell disease. FED is the most common cause of EC dysfunction and is diagnosed by the appearance of drops called *guttae* on the DM situated on the posterior surface of the cornea. Although this technique has been successfully used in the clinic, it is limited to the *en face* 2D image of the cells as well as the small field of view (especially for modern non contact devices) and does not allow accessing information on the microstructure around ECs, which could provide some insights into the mechanism of the disease. Confocal Microscopy (CM) was proposed to overcome these limitations [7–9]. Although the imaging depth of CM may accommodate the endothelial layer on healthy cornea (center thickness ~550 μm), it becomes limited in situations such as FED, where center thickness can reach 1.2 mm. Also, CM is challenged when imaging the posterior periphery of the cornea. Although spectacular larger fields of view have been recently achieved by montaging multiple images [10,11], CM typically offers a smaller field of view within a single frame (about 400 μm × 400 μm), and the difficulty in localizing the axial positioning of the sample under investigation further limits CM imaging of the cornea [12]. Furthermore, the sectioning capability using confocal detection decreases rapidly as a function of depth, thus limiting the use of this technique for imaging ECs *in vivo* [13,14]. Finally, given that the CM generally requires contact with the ocular surface, it is frequently not well tolerated by patients. A non-contact CM approach has been recently investigated, and results pointed to trade-offs in resolution compared to contact CM as well as the inability to determine the depth of acquired images within the cornea [15]. Optical

Coherence Tomography (OCT) is an optical imaging technique that has led to impressive developments during the past decades and is still presenting a great untapped potential for the future [16]. Focused investigations across various application fields are driving the advancement of the capabilities of OCT. For instance, the lateral resolution of conventional OCT instruments is limited to tens of micrometers and hampers the adoption of OCT in a wide range of applications that require cellular resolution comparable to or approaching histology. The numerical aperture (NA) of the optics sets the lateral resolution in the focal plane of the optics and throughout the depth of focus. However, the depth of focus is inversely proportional to NA^2. As a result, OCT typically operates at low NA with a corresponding lateral resolution in the order of 10 to 20 μm, which enables a long depth of focus on the millimeter scale at the expense of lateral resolution. Full field *en face* OCT was proposed as a solution to provide high lateral resolution imaging at the expense of lower volumetric imaging speed and lower sensitivity. Grieve et al. pioneered 3-D imaging of corneal microstructures using full field OCT, where a lateral resolution of ~1 μm with field of view comparable to CM was demonstrated [17]. Optical coherence microscopy (OCM) was introduced to achieve cellular resolution by combining the high axial resolution of OCT and high lateral resolution of confocal microscopy gating to achieve high-contrast imaging of deep layers in tissue [18]. The gain in lateral resolution in OCM is reached at the expense of a limited depth of focus in the order of 100 to 200 μm [19]. Gabor-domain optical coherence microscopy (GD-OCM) was proposed to extend the imaging depth of OCM to the millimeter range while maintaining a constant cellular resolution [20]. A liquid lens was incorporated in a bio-inspired objective to dynamically refocus at different depth locations up to 2 mm to acquire multiple images that are then combined in a single volume, with a constant lateral resolution of 2 μm [21]. The imaging system with micron-class resolution (i.e., 2 μm both laterally and axially) and high-speed processing has been detailed in previous papers [22,23]. In this study, we extended the capabilities of GD-OCM to assess microstructures deep inside the cornea. The system was calibrated in this work for a super-luminescent diode laser with 840 nm center wavelength and 100 nm bandwidth (BroadLighter D-840-HP-I, Superlum®, Ireland), which is out of the wavelength range of the human eye visual sensitivity. For safety requirements, we deliver a power of 1 mW in the sample arm. This power is appropriate to illuminate ECs and is far below the maximum admissible power by ANSI [24]. Furthermore, the beam focused in the cornea is widely spread out on the retina, thus limiting any risk of retinal phototoxicity. Dynamic-focusing of the liquid lens during the acquisition allows imaging different sections of the cornea. For each location, we scanned a field of view of 1 mm × 1 mm, with a lateral sampling interval of 1 μm to exercise the full lateral resolution capability of the system.

The capability of GD-OCM to provide the 3D distribution of corneal microstructures was first investigated and validated using fresh pig eyeballs obtained from a local abattoir. The experiments were performed within three hours postmortem. As shown in Fig. 1, the 3D high definition images of the central porcine cornea, which thickness was measured to be ~850 μm, can be achieved with a field of view of 1 mm × 1 mm. The different layers of the cornea can be distinguished in the x–z cross-sectional image (Fig. 1b). *En face* x–y images at different depths in the cornea also show a corneal nerve, stromal keratocytes, and the posterior layer endothelium with its basement, DM (Fig. 1c–e). In addition, to the best of our

knowledge, this is the first time that a view of ECs is acquired on a field of view of 1 mm × 1 mm using OCT-based technology (Fig. 1f). Such a large field of view is beneficial for increasing the reliability of quantitative analysis of ECs morphology and ECD calculation, which are key factors in the diagnosis of endothelial dystrophies, the evaluation of donor corneas, as well as in the follow up of patients having received a corneal transplantation.

The periphery of the cornea was also explored during this investigation. Figure 2 shows the images of the periphery with distinction of limbal immune cells (Fig. 2a,c), and the peripheral endothelium that includes ECs, the transition zone (TZ), and the trabecular meshwork (TM) (Fig. 2d).

In order to investigate the microstructural changes due to FED, we imaged two different groups of human corneas procured on healthy donors and on patients with FED. All procedures conformed to the tenets of the Declaration of Helsinki for biomedical research involving human subjects. Central corneal buttons of patients with FED were removed during a penetrating keratoplasty procedure and were collected as per the usual protocol in force in our University Hospital and by presumed consent further to the written information given to all admitted patients. This protocol was written by our Hospital's commission for clinical research and innovation and accepted by the local ethics committee (CPP Sud Est I, CHU Saint Etienne, France). Corneas assigned to scientific use were procured from bodies donated to science (Laboratory of Anatomy, Faculty of Medicine) as permitted by French law. Each donor volunteered their body and gave written consent to the Laboratory of Anatomy; no additional approval by the ethics committee was required. Figure 3 shows structural modifications of the extracellular matrix typical of FED. As compared to healthy cornea (Fig. 3a), we observe a thickening of the DM on corneas with FED (Fig. 3b). Figures 3c,e present 2D views of the endothelial layer where *guttae*, characteristic of FED can be observed (Fig. 3e). In addition, the posterior stromal layers of corneas with FED present alteration of keratocytes that are larger in size, number and reflectivity than in normal corneas [Figs. 3(d) and 3(f)]. Whether these observations have etiologic relevance, further investigations may help to clarify these findings and whether there are associated with the course of the disease. Future work will investigate corneas at different stage of the disease in order to provide additional insight into the progression of the disease.

The ability of the system to explore the microstructures around the ECs *in vivo* at the periphery of the cornea offers the possibility to further investigate the proliferation and migration capabilities of ECs – a topic that remains controversial. Recent clinical cases suggested however that the recipient corneal periphery plays an important role in the re-endothelialization of the central cornea after transplantation, supported by the observation of the replacement of donors' ECs by recipients' ECs on the corneal grafts [25]. Full recovery of the corneal transparency has also been reported in the case of complete detachment of the donor endothelial graft [26]. These findings suggest potential cell proliferation at the periphery of the endothelium. Our team recently identified new evidence of proliferation and migration of ECs on excised human corneas [27]. We reported that ECs might proliferate at the extreme periphery and migrate extremely slowly toward the corneal center while forming columns of ECs. During their migration they might deposit collagen that forms centripetal radial furrows visible in the periphery. These microstructures were discovered

thanks to *en face* observation of *ex vivo* corneas using optical and electron microscopy. In order to further assess this hypothesis, we need to measure *in vivo* the length of these radial furrows and/or centripetal cells rows in peripheral corneas of healthy subject of different ages. GD-OCM will be used to investigate these features first on human excised corneas and secondly *in vivo*.

In conclusion, we reported in this paper on the ability of GD-OCM to resolve the microstructures of the cornea, *ex vivo.* This demonstration opens a wide range of applications. For instance, the screening of corneal grafts received by corneal banks is critical to detecting abnormalities of the corneal endothelium (cells density, evidence of *guttae*, etc.) and of the stroma (infraclinic opacity, LASIK interface, etc.). Future work aims at *in vivo* investigation of the different aspects of corneal bioengineering considered as a fundamental component in tomorrow's treatment for the most severe epithelial, stromal and endothelial diseases. A better understanding of *in vivo* ECs microanatomy through non-invasive imaging is crucial to identify anomalies at the early stage of FED, before the disease become symptomatic. Adoption in ophthalmology of this advanced imaging modality that achieves cellular resolution deep in corneal tissues may bring new perspectives in the diagnosis and follow-up of corneal diseases.

Acknowledgments

This research was funded by the NYSTAR Foundation (C050070), a Center for Visual Science NIH Training grant to Tankam (EY007125), and a NSF STTR Phase I grant awarded to LighTopTech Corp. (ENG 1346453).

References

1. Cox JL, Farrell RA, Hart RW, Langham ME. J Physiol. 1970; 210:601–616. [PubMed: 5499815]
2. Maurice DM. J Physiol. 1957; 136:263–286. [PubMed: 13429485]
3. Bourne WM, Kaufman HE. Am J Ophthalmol. 1976; 81(3):319–323. [PubMed: 1258956]
4. Van Horn DL, Sendele DD, Seideman S, Buco PJ. Invest Ophthalmol Vis Sci. 1977; 16(7):597–613. [PubMed: 873721]
5. Sturrock GD, Sherrard ES, Rice NS. British J Ophthalmol. 1978; 62(12):809–814.
6. Kiuchi T, Tatsuzaki H, Hommura S, Oshika T. Eye. 2004; 18(9):929–934. [PubMed: 15002020]
7. Chiou AG, Kaufman SC, Beuerman RW, Ohta T, Soliman H, Kaufman HE. British J Ophthalmol. 1999; 83(2):185–189.
8. Parmar DN, Awwad ST, Petroll WM, Bowman RW, McCulley JP, Cavanagh HD. Ophthalmol. 2006; 113(4):538–547.
9. Erie JC, McLaren JW, Patel SV. Am J Ophthalmol. 2009; 148(5):639–646. [PubMed: 19674730]
10. Edwards K, Pritchard N, Gosschalk K, Sampson GP, Russell A, Malik RA, Efron N. Cornea. 2012; 31(9):1078–1082. [PubMed: 23045727]
11. Turuwhenua JT, Patel DV, McGhee CNJ. Invest Ophthalmol Vis Sci. 2012; 53:2235–2242. [PubMed: 22427563]
12. Niederer RL, McGhee CNJ. Prog Ret Eye Res. 2010; 29(1):30–58.
13. Patel SV, McLaren JW, Hodge DO, Bourne WM. Invest Ophthalmol Vis Sci. 2002; 43(4):995–1003. [PubMed: 11923239]
14. Kaufman SC, Musch DC, Belin MW, Cohen EJ, Meisler DM, Reinhart WJ, Van Meter WS. Ophthalmol. 2004; 111(2):396–406.
15. Pritchard N, Edwards K, Efron N. Contact Lens Ant Eye. 2014; 37(1):44–48.
16. Drexler W, Liu M, Kumar A, Kamali T, Unterhuber A, Leitgeb RA. J Biomed Opt. 2014; 19(7): 071412. [PubMed: 25079820]

17. Grieve K, Pâques M, Dubois A, Sahel J, Boccara C, Le Gargasson JF. Invest Ophthalmol Vis Sci. 2004; 45(11):4126–4131. [PubMed: 15505065]
18. Izatt JA, Hee MR, Owen GM, Swanson EA, Fujimoto JG. Opt Lett. 1994; 19:590. [PubMed: 19844382]
19. Aguirre AD, Hsiung P, Ko TH, Hart I, Fujimoto JG. Opt Lett. 2003; 28(21):2064–2066. [PubMed: 14587816]
20. Rolland JP, Meemon P, Murali S, Thompson KP, Lee KS. Opt Express. 2010; 18(4):3632–3642. [PubMed: 20389373]
21. Murali S, Thompson KP, Rolland JP. Opt Lett. 2009; 34(2):145–147. [PubMed: 19148236]
22. Lee KS, Thompson KP, Meemon P, Rolland JP. Opt Lett. 2011; 36(12):2221–2223. [PubMed: 21685973]
23. Tankam P, Santhanam AP, Lee KS, Won J, Canavesi C, Rolland JP. J Biomed Opt. 2014; 19(7): 071410.
24. American National Standards Institute. American national standard for safe use of lasers, ANSI Z136. 2007:1–2007.
25. Lagali NS, Stenevi U, Claesson M, Fagerholm P, Hanson C, Weijdegård B, Strömbeck AS. and Swedish Society of Cornel Surgeons. Invest Ophthalmol Vis Sci. 2010; 51:1898. [PubMed: 19815734]
26. Dirisamer M, Yeh RY, Van Dijk K, Ham L, Dapena I, Melles GR. Am J Ophthalmol. 2012; 154:290–296. [PubMed: 22633346]
27. He Z, Campolmi N, Gain P, Ha Thi BM, Dumollard JM, Duband S, Peoc'h M, Piselli S, Garraud O, Thuret G. Stem Cells. 2012; 30(11):2523–2534. [PubMed: 22949402]

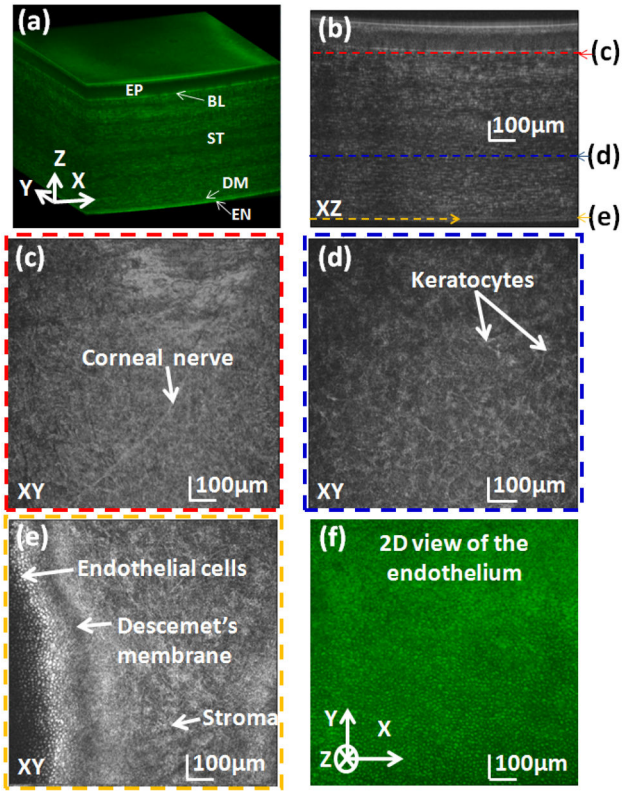

Fig. 1.

Imaging of the central cornea of a porcine eyeball. (a) 3D high definition image of the full center cornea and (b) cross-sectional x–z image showing the different layers of the cornea. *En face* x–y images at different depth of the cornea show a corneal nerve (c), stromal keratocytes (d) and the posterior layer including the DM and ECs (e), 2D view of ECs obtained by a projection of the 3D volume along z direction (looking from the back of the cornea) is shown in (f).

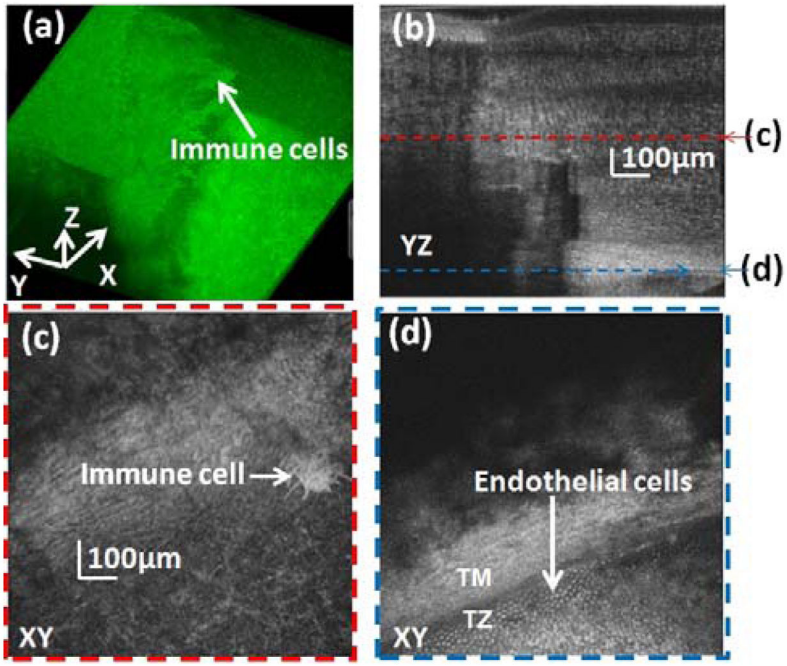

Fig. 2.

Imaging of the periphery of the porcine cornea. (a) 3D view of the corneal periphery with good distinction of limbal immune cells, presumably Langerhans or dendritic cells as ball-like structures with strand-like dendritic attachments (c), (b) cross-sectional x–z image of the corneal periphery, (d) peripheral endothelium including ECs, TZ and TM.

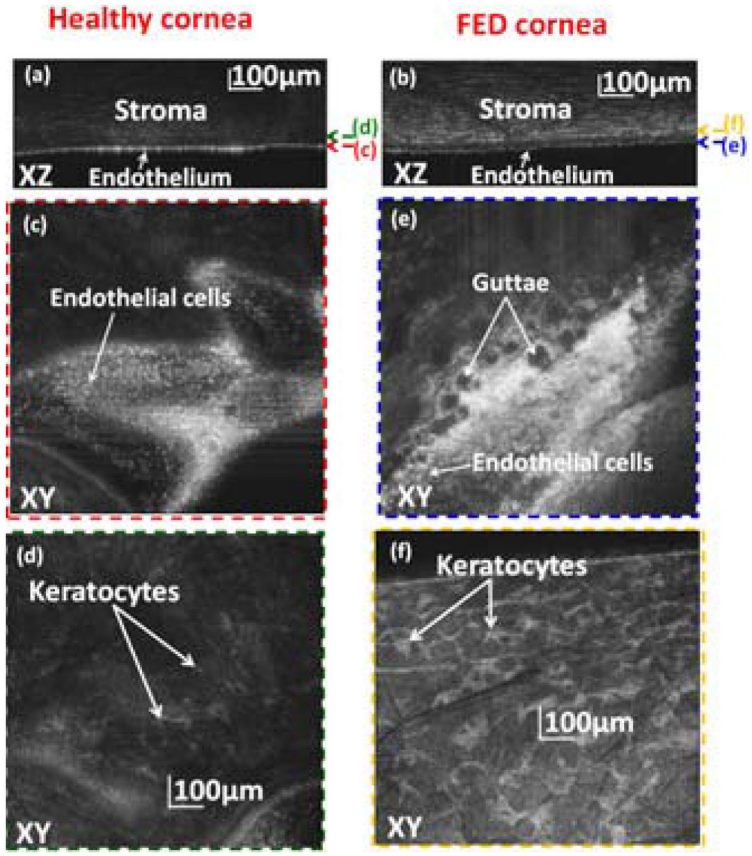

Fig. 3.

Structural investigation of the posterior layers of human corneas of healthy versus FED corneas. Both specimens were fixed with the same protocol. (a) and (b) present cross-sectional images of healthy and FED corneas, respectively, while (c–f) show the comparison of the *en face* x–y images around the endothelium layer.